

**Sea ice cover in  
Isfjorden and  
Hornsund 2000–2014  
by using remote  
sensing**

S. Muckenhuber et al.

# Sea ice cover in Isfjorden and Hornsund 2000–2014 by using remote sensing

S. Muckenhuber<sup>1</sup>, F. Nilsen<sup>2,3</sup>, A. Korosov<sup>1</sup>, and S. Sandven<sup>1</sup>

<sup>1</sup>Nansen Environmental and Remote Sensing Center (NERSC), Thormøhlensgate 47, 5006 Bergen, Norway

<sup>2</sup>University Centre in Svalbard (UNIS), P.O. Box 156, 9171 Longyearbyen, Norway

<sup>3</sup>Geophysical Institute, University of Bergen, P.O. Box 7800, 5020 Bergen, Norway

Received: 22 June 2015 – Accepted: 8 July 2015 – Published: 31 July 2015

Correspondence to: S. Muckenhuber (stefan.muckenhuber@nersc.no)

Published by Copernicus Publications on behalf of the European Geosciences Union.

Title Page

Abstract

Introduction

Conclusions

References

Tables

Figures

⏪

⏩

◀

▶

Back

Close

Full Screen / Esc

Printer-friendly Version

Interactive Discussion

## Abstract

A satellite database including 16 555 satellite images and ice charts displaying the area of Isfjorden, Hornsund and the Svalbard region has been established with focus on the time period 2000–2014. 3319 manual interpretations of sea ice conditions have been conducted, resulting in two time series dividing the area of Isfjorden and Hornsund into “Fast ice”, “Drift ice” and open “Water”. The maximum fast ice coverage of Isfjorden is > 40 % in the periods 2000–2005 and 2009–2011 and stays < 30 % in 2006–2008 and 2012–2014. Fast ice cover in Hornsund reaches > 40 % in all considered years, except for 2012 and 2014, where the maximum stays < 20 %. The mean seasonal cycles of fast ice in Isfjorden and Hornsund show monthly averaged values of less than 1 % between July and November and maxima in March (Isfjorden, 35.7 %) and April (Hornsund, 42.1 %) respectively. A significant reduction of the monthly averaged fast ice coverage is found when comparing the time periods 2000–2005 and 2006–2014. The seasonal maximum decreases from 57.5 to 23.2 % in Isfjorden and from 52.6 to 35.2 % in Hornsund. A new concept, called “days of fast ice coverage” (DFI), is introduced for quantification of the interannual variation of fast ice cover, allowing for comparison between different fjords and winter seasons. Considering the time period from 1 March until end of sea ice season, the mean DFI values for 2000–2014 are  $33.1 \pm 18.2$  DFI (Isfjorden) and  $42.9 \pm 18.2$  DFI (Hornsund). A distinct shift to lower DFI values is observed in 2006. Calculating a mean before and after 2006 yields a decrease from 50 to 22 DFI for Isfjorden and from 56 to 34 DFI for Hornsund.

## 1 Introduction

Svalbard is an Arctic archipelago located between 76–81° N and 10–34° E. It is surrounded by the Arctic Ocean in the north, with Greenland Sea and Fram Strait to the west and the Barents Sea to the east. Spitsbergen is the largest island in the

## Sea ice cover in Isfjorden and Hornsund 2000–2014 by using remote sensing

S. Muckenhuber et al.

Title Page

Abstract

Introduction

Conclusions

References

Tables

Figures

◀

▶

◀

▶

Back

Close

Full Screen / Esc

Printer-friendly Version

Interactive Discussion



archipelago and the study area of this work includes the fjords along the west coast of Spitsbergen.

Water masses along the west side of Spitsbergen are strongly influenced by the West Spitsbergen Current (WSC), that is steered along the slope between the West Spitsbergen Shelf and the deep ocean, the coastal current (CC) on the shelf, and freshwater input from glacier and river runoff along the coastline. The WSC transports warm and salty Atlantic Water (AW) northward, representing the major oceanic heat and salt source for the Arctic Ocean. It is a strong contribution to Svalbard's relatively warm climate and makes Fram Strait the northernmost permanently ice-free ocean. The fjords along western Spitsbergen are usually separated from the WSC by the colder and fresher water masses of the northward flowing CC. This, in combination with low temperatures and fresh water input from glacier and river runoff, makes seasonal sea ice growth inside the fjords possible. But AW from the WSC can reach the upper shelf and eventually flood into the fjords (Nilsen et al., 2008, 2012). These warm water intrusions have a strong effect on the seasonal sea ice cover inside the fjords. The fjord-shelf exchange is controlled by the density difference between the fjord water masses and the AW, which is determined by the sea ice and brine production during winter (Nilsen et al., 2008). This means, that the sea ice cover inside the fjords is not only a result of advected or advecting water masses, but can alter the fjord water significantly and influence the exchange with the shelf.

The aim of this study is to investigate sea ice conditions between 2000–2014 in two representative fjords along the west coast of Spitsbergen, where ocean and atmosphere data are available for further analysis. The two considered fjords are Isfjorden, the largest fjord of Spitsbergen with its 2490 km<sup>2</sup>, and Hornsund, a smaller fjord (320 km<sup>2</sup>) located in southern Spitsbergen (areas defined with ArcGIS and Landsat 8 images from 2013). Both fjords reveal a seasonal sea ice coverage with strong variations between different years. Information about sea ice coverage in Isfjorden has been collected between 1974 until 2008 in Grønfjorden (Zhuravskiy et al., 2012), which is a small sub fjord at the southern entrance of Isfjorden, but no data considering the

## Sea ice cover in Isfjorden and Hornsund 2000–2014 by using remote sensing

S. Muckenhuber et al.

Title Page

Abstract

Introduction

Conclusions

References

Tables

Figures

◀

▶

◀

▶

Back

Close

Full Screen / Esc

Printer-friendly Version

Interactive Discussion



## Sea ice cover in Isfjorden and Hornsund 2000–2014 by using remote sensing

S. Muckenhuber et al.

Title Page

Abstract

Introduction

Conclusions

References

Tables

Figures

◀

▶

◀

▶

Back

Close

Full Screen / Esc

Printer-friendly Version

Interactive Discussion

entire fjord area has been published so far. Sea ice conditions in Hornsund were investigated during the winter seasons 2005 to 2011 (Styszyńska and Kowalczyk, 2007; Styszyńska and Rozwadowska, 2008; Styszyńska, 2009; Kruszewski, 2010, 2011, 2012). In-situ observations from the Polish Polar Station in Isbjørnhamna, a bay at the northern entrance of Hornsund, were compared with atmospheric and oceanic measurements. The survey concentrates on regional ice conditions near Isbjørnhamna and no time series for the entire fjord is given.

The data for this article was collected and interpreted within the framework of the Polish-Norwegian AWAKE-2 project. The aim of AWAKE-2 is to understand the interactions between the main components of the climate system in the Svalbard area: ocean, atmosphere and ice to identify mechanisms of interannual climate variability and long-term trends. The main hypothesis is that the AW inflows over the Svalbard shelf and into the fjords have become more frequent during the last decades and this results in new regimes and changes in atmosphere, ocean, sea ice and glaciers in Svalbard. Being a link between land and ocean, Arctic fjords are highly vulnerable to warming and are expected to exhibit the earliest environmental changes resulting from anthropogenic impacts on climate. Sea ice cover is a key parameter for monitoring climate variability and trends, since it captures the variability of both ocean and atmosphere conditions. Due to the major role sea ice cover plays in air–sea interactions, knowledge about the ice cover is crucial for a better understanding of the Arctic fjord system.

The paper is organised as follows: Sect. 2 explains the collected satellite images and gives an error estimate for the established sea ice cover time series. A method for manual interpretation of satellite data to describe sea ice conditions in a fjord is introduced in Sect. 3 as well as a new index for quantifying fast ice coverage in a fjord. The sea ice cover time series for Isfjorden and Hornsund, the resulting DFI values and the dates for onset of freezing are presented in Sect. 4. The discussion can be found in Sect. 5.

## 2 Data

Investigating sea ice conditions via satellite remote sensing in comparable small areas like Isfjorden and Hornsund requires a spatial resolution of a few 100 m or lower. Daily images throughout the year with this resolution are only produced by Synthetic Aperture Radar (SAR), which is an active microwave sensor capable of penetrating cloud cover and taking images during polar night. Since the interpretation of sea ice conditions from SAR images can be ambiguous, high and medium resolution visual/near infrared (VIS/NIR) images provide valuable additional information during polar day. They can also be utilised, if SAR images are not available. However, good temporal coverage with VIS/NIR sensors is only achieved with a resolution above 250 m. Hence, lower accuracy is expected if only VIS/NIR images are concerned.

A satellite database including 6571 SAR images, 9123 VIS/NIR images and 861 ice charts displaying the area of Isfjorden and Hornsund has been established (see Table 1). Focus was put on the time period 2000 until 2014 and the part of the season during sea ice is present in the fjords.

NERSC maintains a large satellite database including several thousand Level 1 SAR images from ASAR (Advanced Synthetic Aperture Radar on ENVISAT) and Radarsat-2. To select the images which are recorded at the considered region and time period, the NERSC MAIRES online service (<http://web.nersc.no/project/maires/sadweb.py>) has been used. 4326 ASAR and 2245 Radarsat-2 sub images covering Isfjorden and Hornsund respectively have then been created and stored in GeoTIFF format. The collected SAR data represent a time series from 2005 until 2014 with a temporal resolution of around 1–2 images per day.

Medium resolution VIS/NIR images from MERIS (Medium Resolution Imaging Spectrometer on ENVISAT) and MODIS (Moderate Resolution Imaging Spectroradiometer on Terra and Aqua) covering the Svalbard region have been downloaded from websites hosted by NASA (National Aeronautics and Space Administration). MODIS images can be ordered pre-processed, which allows to download all available images of the con-

### Sea ice cover in Isfjorden and Hornsund 2000–2014 by using remote sensing

S. Muckenhuber et al.

Title Page

Abstract

Introduction

Conclusions

References

Tables

Figures

◀

▶

◀

▶

Back

Close

Full Screen / Esc

Printer-friendly Version

Interactive Discussion

sidered area and time period. A total of 8501 MODIS images represents a temporal resolution of up to several images per day for the period 2000 until 2014. The relevant MERIS images had to be chosen prior to downloading via online quicklooks to select images with cloud free conditions. About 10 MERIS images per year have been chosen and added to the database.

High resolution VIS/NIR images have a distinct lower spatial and temporal coverage, but when available, view the ice conditions with an unmistakable clarity. 335 images from Landsat 1–8 and 161 from ASTER (Advanced Spaceborne Thermal Emission and Reflection Radiometer on Terra) have been chosen for downloading via quicklooks provided by USGS (United States Geological Survey) and the Japan Space System.

In addition to the satellite images, 861 ice charts from the Norwegian Meteorological Institute (met.no) have been added to the database. These ice charts are based on the same satellite images that are used for this paper. The resolution of the met.no ice charts is too low to give sufficient accurate estimates about daily ice conditions in fjords like Isfjorden and Hornsund. Nevertheless, the met.no charts can serve as additional information about the overall ice situation outside the boundary of the high resolution SAR image. Most of the stored ice charts depict ice conditions during polar night when no visual images are available to get a quick overview of the large scale ice situation.

### Error estimate

Since the time series is based on manual interpretation, defining an exact error value is not possible. Nevertheless, possible error sources can be evaluated and an error estimate from the analysing sea ice expert can be given.

The biggest error source is wrong interpretation of ambiguous SAR images during polar night, when no VIS/NIR images are available for validation. “Fast ice” is generally more distinct, whereas the separation of “Drift ice” and open “Water” is sometimes inconclusive. An error source important for the time series before 2005, is the lower resolution of MODIS and MERIS data. This has less influence on the reliability, but effects the accuracy of the daily values. Minor errors influencing the accuracy are in-

## Sea ice cover in Isfjorden and Hornsund 2000–2014 by using remote sensing

S. Muckenhuber et al.

Title Page

Abstract

Introduction

Conclusions

References

Tables

Figures



Back

Close

Full Screen / Esc

Printer-friendly Version

Interactive Discussion



## Sea ice cover in Isfjorden and Hornsund 2000–2014 by using remote sensing

S. Muckenhuber et al.

Title Page

Abstract

Introduction

Conclusions

References

Tables

Figures

◀

▶

◀

▶

Back

Close

Full Screen / Esc

Printer-friendly Version

Interactive Discussion



sufficient geographic information of the satellite image, which can lead to a slightly stretched satellite image compared to the fjord polygon, and the changing coastline due to glacier retreat. The glacier retreat has a negligible effect on larger fjords like Isfjorden, but can change the total area of smaller fjords like Hornsund in the order of percent. A strong retreat of the glaciers surrounding Hornsund was detected between 2000 and 2014.

The daily value error estimate based on consideration of the mentioned sources and personal appraisal of the analysing sea ice expert is in the order of a few percent for “Fast ice” and between several percent up to 10 % for “Drift ice” and open “Water” depending on the availability of VIS/NIR images for validation. The error propagation from a single day to a time period of several months leads to a very high accuracy for all given days of fast ice coverage (DFI) values.

### 3 Method

The downloaded Level 1 satellite data from ASAR, Radarsat-2, MODIS and MERIS were processed with the open-source python toolbox “Nansat” (developed by NERSC) into geoTIFF and PNG Level 2 images, which can be displayed by ArcGIS and several other programs. Within ArcGIS, two polygons covering Isfjorden and Hornsund were created by using a high resolution VIS/NIR image from Landsat 8 as reference. This polygon describes the fjord area very accurately and can be cut into pieces in order to evaluate the sea ice coverage by area. Due to the large amount of considered days and images, the processing chain needs to be fast and efficient. This is achieved by implementing most steps into a python code working inside ArcGIS.

For the time period 2005–2014, both SAR and VIS/NIR images are available and the processing chain for a specific date (leading to one data point in the time series) is as followed: The SAR images of the considered day are loaded into ArcGIS and their symbology is adjusted to increase the visual difference between water and ice. Then the mentioned polygon is put on top of the images and cut by a sea ice expert into the

regions “Fast ice”, “Drift ice” and open “Water” (Fig. 1). The origin of the sea ice, which can be both freezing inside the fjord or advection from the shelf, is not considered during the manual interpretation. The area of each region is calculated in m<sup>2</sup> using a built in function of ArcGIS and the results are saved in a text file. In case VIS/NIR images are available for the same date, they are used for validation and interpretation support of the SAR images.

Prior 2005, no high quality SAR images could be accessed and the time series is solely based on VIS/NIR images. During polar night it is therefore not possible to describe the ice conditions. During polar day high accuracy is only achieved for days with high resolution VIS/NIR images and lower accuracy is expected for the other days, due to the lower resolution of MODIS and MERIS compared to SAR. The method yields still high reliability for the analysed years before 2005, since water and ice can be separated unmistakable on visual images. Continuity of the time series is expected, since MODIS, Aster and Landsat data is available and considered for the entire time series.

### Days of fast ice coverage

To quantify sea ice coverage in a defined region (in our case Isfjorden and Hornsund), a new concept called “Days of fast ice coverage” (DFI) is introduced. The index describes fast ice conditions over a considered time period in a single value with unit days. Both temporal and spatial extent of the fast ice is included. The DFI are calculated by building the sum over the fast ice area of all considered days relative to the total area, i.e. in our case the entire fjord area (Eq. 1).

$$DFI = \sum_{\text{days}} \frac{\text{fast ice area}}{\text{total area}} \quad (1)$$

The DFI values allow a simple comparison between different regions and time periods and with external parameter like atmospheric or oceanic data.

## Sea ice cover in Isfjorden and Hornsund 2000–2014 by using remote sensing

S. Muckenhuber et al.

Title Page

Abstract

Introduction

Conclusions

References

Tables

Figures

◀

▶

◀

▶

Back

Close

Full Screen / Esc

Printer-friendly Version

Interactive Discussion



## 4 Results

By utilising the created satellite database (Sect. 2) and applying the described method (Sect. 3), two time series dividing the area of Isfjorden and Hornsund into “Fast ice”, “Drift ice” and open “Water” have been created (Figs. 2 and 3). In total, 3319 manual interpretations of sea ice conditions were conducted by a sea ice expert, leading to an almost daily resolution between 2000 and 2014. Unclassified gaps occur in both time series when SAR images were unavailable during the dark season (white gaps in Figs. 2 and 3).

The daily surface coverage in Isfjorden between 2000 and 2014 is shown in Fig. 2. A maximum fast ice coverage of 40 % and higher is reached in the time periods 2000–2005 and 2009–2011. During the periods 2006–2008 and 2012–2014, the fast ice area stays always below 30 %. Figure 3 displays the daily surface coverage in Hornsund for 2000 until 2014. Maximum fast ice cover values above 40 % are reached in all years, except for 2012 and 2014, where the fast ice season is significantly shorter and the maximum stays below 20 %. Late growth of fast ice is also observed in 2006, 2008 and 2013.

Monthly averaged fast ice cover, based on the time series shown in Figs. 2 and 3, are shown in Figs. 4 and 5, respectively. The monthly averaged values display the seasonal cycle of fast ice growth and melt/break up in Isfjorden and Hornsund. Values for the dark season (November–February) before 2006 are missing, since no high quality SAR images were available for this period.

Less than 1 % monthly averaged fast ice cover were observed in Isfjorden between July and November (Fig. 4). Considering the mean over the entire observation period 2000–2014 (black line, Fig. 4), the highest value with 35.7 % is reached in March. Before 2005 (blue line, Fig. 4), the peak in March is 57.5 %. The mean for 2006–2014 (red line, Fig. 4) shows the highest value with 23.2 % in April. Monthly averaged fast ice coverage in Hornsund is shown in Fig. 5. Less than 2 % fast ice is observed between July and November. April is the month with the highest fast ice coverage values: 42.1 %

### Sea ice cover in Isfjorden and Hornsund 2000–2014 by using remote sensing

S. Muckenhuber et al.

Title Page

Abstract

Introduction

Conclusions

References

Tables

Figures



Back

Close

Full Screen / Esc

Printer-friendly Version

Interactive Discussion



for the mean over all considered years (black line, Fig. 5), 52.6% for the period 2000–2005 (blue line, Fig. 5) and 35.2% for 2006–2014 (red line, Fig. 5). Comparing the time periods 2000–2005 and 2006–2014 yields a significant reduction of the monthly averaged fast ice coverage. The seasonal maximum decreases by 60.2 and 33.1% (relative to the value for 2000–2005) in Isfjorden and Hornsund respectively.

#### 4.1 Days of fast ice coverage (DFI)

Utilising Eq. (1) and the time series shown in Figs. 2 and 3, DFI values have been calculated for Isfjorden and Hornsund and the results are shown in Table 2. For each sea ice season, two different time periods were considered. The “total season” refers to the entire sea ice season, which lasts usually from November of the previous year until June, and the “short season” lasts from 1 March until the end of the sea ice season. The “short season” can also be calculated for years where only VIS/NIR images are available, whereas SAR images are necessary for the “total season”.

High correlation coefficients ( $R$ ) between the total and short season for both Isfjorden ( $R = 0.89$ ) and Hornsund ( $R = 0.94$ ) suggest that the short season values capture well the interannual variability of the entire season. Only the ice season 2011 shows a higher difference in the short and total season DFI values (Table 2), due to very early fast ice growth (Fig. 6) and a high fast ice peak before March.

The DFI mean values (total and short season, Table 2) for Isfjorden are around 10 DFI lower than the mean values for Hornsund, which means around 25% less fast ice coverage in Isfjorden relative to the total area of each fjord. Similar high standard deviations for both fjords express strong variations between different years.

Both “short season” time series show a strong decrease in 2006. Isfjorden’s DFI values between 2000 and 2005 are all above the mean, whereas after 2006 only 2009 has more than the average days of fast ice coverage. Calculating a mean before and after 2006 shows a drop from 50 to 22 DFI. The situation of Hornsund is similar, yet not so pronounced. The mean value decreases from 56 to 34 DFI before and after 2006.

## Sea ice cover in Isfjorden and Hornsund 2000–2014 by using remote sensing

S. Muckenhuber et al.

Title Page

Abstract

Introduction

Conclusions

References

Tables

Figures

◀

▶

◀

▶

Back

Close

Full Screen / Esc

Printer-friendly Version

Interactive Discussion



Low values are reached in 2006 and particularly in 2012 and 2014, where the fast ice coverage goes down to almost 0 DFI.

## 4.2 Onset of freezing

The sea ice season in Isfjorden and Hornsund starts usually between late autumn and beginning of winter. Figure 6 shows the days with first appearance of drift and fast ice, i.e. the start of the sea ice season in Isfjorden and Hornsund. The year refers to the winter season, which starts during the previous year. This means, that January in Fig. 6 refers to the beginning of the respective year. The first sea ice of the season appears during polar night and SAR images are necessary to define the date of the freezing onset. Since no SAR images were available prior 2005, the time series in Fig. 6 starts with the sea ice season 2006. Too few satellite images have been available to give an reliable estimate of the freezing onset in Isfjorden 2007.

Drift ice starts to grow in Isfjorden in all examined years around the beginning of November. The appearance of fast ice in Isfjorden varies between mid November (2011), December and beginning of January (2008, 2013 and 2014). The start of the sea ice season in Hornsund underlays stronger variations. The first drift ice of the season was found in November or December in all years except for the last two years, during which an early start in October was observed. Fast ice starts to appear in Hornsund between the end of November and mid March. Late fast ice formation was observed during 2006, 2008 and 2013.

## 5 Discussion and outlook

Isfjorden has two periods with more sea ice (2000–2005 and 2009–2011, Fig. 2) and two periods with less sea ice cover (2006–2008 and 2012–2014, Fig. 2). All periods last 3 years or more, which suggests the involvement of an oceanic mechanism since the atmospheric conditions underlay variations with shorter time scales. However, wind

### Sea ice cover in Isfjorden and Hornsund 2000–2014 by using remote sensing

S. Muckenhuber et al.

Title Page

Abstract

Introduction

Conclusions

References

Tables

Figures

⏪

⏩

◀

▶

Back

Close

Full Screen / Esc

Printer-friendly Version

Interactive Discussion



## Sea ice cover in Isfjorden and Hornsund 2000–2014 by using remote sensing

S. Muckenhuber et al.

Title Page

Abstract

Introduction

Conclusions

References

Tables

Figures

◀

▶

◀

▶

Back

Close

Full Screen / Esc

Printer-friendly Version

Interactive Discussion

forcing of the West Spitsbergen Shelf (WSS) on timescales from days to months is shown to be one of the mechanisms of starting a shelf circulation of warm AW towards the fjords (Cottier et al., 2007; Nilsen et al., 2012). Cottier et al. (2007) reported that during the Arctic winter of 2005/2006, periods of sustained along-shelf winds generated upwelling and cross-shelf exchange that caused extensive flooding of the coastal waters with warm Atlantic Water from the West Spitsbergen Current (WSC) (Cottier et al., 2007). The winter temperature of the WSS reverted to that typical of fall, interrupting the normal cycle of sea ice formation in the region, including both the shelf and the fjords along the west coast of Spitsbergen. Ongoing hydrographic measurement programs and construction of longer time series (Pavlov et al., 2013) show that fjord systems along west Spitsbergen went from an Arctic state to a more Atlantic water state after winter 2006, which is reflected in our sea ice time series. Hence, the sea ice time series in Sect. 4 show that the effect of forcing event on the time scale of weeks, and a corresponding advection of AW, can have an influence on the fjord thermodynamics and local sea ice condition on a yearly time-scale.

Another possible explanation for the perennial duration of both small and large fast ice cover years in Isfjorden can be given by looking at the density difference between the fjord water masses and the AW. In contrast to the external forcing mechanism suggested above, this represents a local forcing mechanism through air–ice–ocean interaction. Nilsen et al. showed that a high ice production during winter, results in a higher formation of dense brine-enriched fjordwater and the local water masses in the fjord proper can end up being denser than the water masses residing on the shelf (Nilsen et al., 2012). This is a key mechanism that enables AW to penetrate into Isfjorden in spring and the following summer and autumn, and determines in which depth the warm AW will circulate in the water column. Considering Isfjorden as a coastal polynya with the opening area restricted by fast ice cover, more sea ice is produced in winters with less fast ice coverage. Hence, low fast ice coverage can cause AW intrusion in the following summer, which then can lead to low fast ice coverage in the following winter if the intruding AW is circulating high in the water column.

## Sea ice cover in Isfjorden and Hornsund 2000–2014 by using remote sensing

S. Muckenhuber et al.

Title Page

Abstract

Introduction

Conclusions

References

Tables

Figures

◀

▶

◀

▶

Back

Close

Full Screen / Esc

Printer-friendly Version

Interactive Discussion



The mechanisms described for Isfjorden could apply for Hornsund, but being a smaller fjord, variations on shorter time scales can be expected. Comparing the time series in Figs. 2 and 3, we see that the interannual variability in sea ice cover in Hornsund, compared to the sea ice cover in Isfjorden, is less influenced by intrusion of AW residing on the shelf. However, Hornsund responds similarly to Isfjorden during the most extreme years of AW dominance on the WSS and strong external forcing mechanisms (Nilsen et al., 2015), i.e. the winters of 2006, 2012 and 2014. Thus, Hornsund, being the most southern fjord along the west coast of Spitsbergen, can serve as an indicator of AW dominance for all fjords north of Hornsund along the west coast. Ocean and atmosphere measurements from the Polish research station in Hornsund carried out by the ongoing Polish-Norwegian project AWAKE-2 (Arctic climate system study of ocean, sea ice and glaciers interactions in Svalbard area) will be utilized to explain the difference between average seasons and years with distinct less sea ice coverage, i.e. 2006, 2012 and 2014.

Considering the start of the freezing season, i.e. the first appearance of drift or fast ice in the two fjords, Isfjorden shows in general less variability and earlier ice growths (Fig. 6). A low correlation between the start of the freezing season for the two fjords is observed, suggesting a stronger dependence on local conditions rather than a large-scale ocean and/or atmosphere influence. Occurrence of drift ice always precedes fast ice, often with a time lead of 1–2 months. However, care must be taken when defining the start of the freezing in Arctic fjords by using satellite images since the first appearance of drift ice will not necessarily reflect that the surface layer of the fjord proper has reached the freezing point temperature, but merely that some protected side fjord within the larger fjord system have a fresher and colder surface layer that are able to produce sea ice for a limited period. Hence, the true freezing season will start somewhere between the first detection of drift ice and the establishment of fast ice in an Arctic fjord.

Recent observations of the ice cover to the north of Svalbard further demonstrate the intimate link between the heat of the Atlantic water and the distribution of sea ice.

## Sea ice cover in Isfjorden and Hornsund 2000–2014 by using remote sensing

S. Muckenhuber et al.

Title Page

Abstract

Introduction

Conclusions

References

Tables

Figures

◀

▶

◀

▶

Back

Close

Full Screen / Esc

Printer-friendly Version

Interactive Discussion



Onarheim et al. (2014) have shown that the sea ice area north of Svalbard has been decreasing for all months since 1979 with the largest ice reduction occurring during the winter months at a rate of 10% per decade (Onarheim et al., 2014). This is in contrast to the observed changes in more central parts of the Arctic Ocean, where largest ice decline is happening during summer. However, the observed reduction is concurrent with a gradual warming of 0.3 °C per decade warming of the AW along West Spitsbergen, and thus, the extra oceanic heat has been the major driver of the sea ice loss, which is concurrent with our results from both Isfjorden and Hornsund. Another indication of warm water as a major is the delayed maximum fast ice area in Isfjorden (Fig. 4) from March to April for the 2000–2005 period to the 2006–2014 period, respectively. A warmer water column in late autumn can cause delayed ice formation and consequently lower ice concentrations in early winter.

In conclusion, the presented sea ice time series serve for a better understanding of interannual variability in Arctic fjord system. Since a sea ice cover reflects the physical state of the ocean and atmosphere, the present sea ice time series can be used to better understand air–ice–ocean interaction processes within each fjord systems, but also in various climate effect studies linked to e.g. glacier dynamics, ocean chemistry and marine biology.

*Acknowledgements.* This research was supported by the Polish-Norwegian AWAKE-2 (Arctic climate system of ocean, sea ice and glaciers interaction in Svalbard) project (Pol-Nor/198675/17/2013). We thank the developer group of the open-source python toolbox “Nansat” (<https://github.com/nanscenter/nansat>) and the following agencies/institutes for providing the utilised satellite images and ice charts: National Aeronautics and Space Administration, European Space Agency, Canadian Space Agency and Norwegian Meteorological Institute.

## References

- Cottier, F., Nilsen, F., Inall, M. E., Gerland, S., Tverberg, V., and Svendsen, H.: Wintertime warming of an Arctic shelf in response to large-scale atmospheric circulation, *Geophys. Res. Lett.*, 34, L10607, doi:10.1029/2007GL029948, 2007. 4054
- 5 Kruszewski, G.: Ice condition in Hornsund (Spitsbergen) during winter season 2008–2009, *Problemy Klimatologii Polarnej*, 20, 187–196, 2010. 4046
- Kruszewski, G.: Ice condition in Hornsund during winter season 2009–2010 (SW Spitsbergen), *Problemy Klimatologii Polarnej*, 21, 229–239, 2011. 4046
- 10 Kruszewski, G.: Ice condition in Hornsund and adjacent waters (Spitsbergen) during winter season 2010–2011, *Problemy Klimatologii Polarnej*, 22, 69–82, 2012. 4046
- Nilsen, F., Cottier, F., Skogseth, R., and Mattsson, S.: Fjord-shelf exchanges controlled by ice and brine production: the interannual variation of Atlantic water in Isfjorden, Svalbard, *Cont. Shelf. Res.*, 28, 1838–1853, 2008. 4045
- 15 Nilsen, F., Vaardal-Lunde, J., and Skogseth, R.: Topographically controlled flow on the West Spitsbergen Shelf with special emphasis on the Atlantic water transport towards Isfjorden, D:07, ICES CM, 2012. 4045, 4054
- Nilsen, F., Skogseth, R., Vaardal-Lunde, J., and Inall, M.: A simple shelf circulation model – intrusion of Atlantic water on the West Spitsbergen Shelf, *J. Phys. Oceanogr.*, submitted, 2015. 4055
- 20 Onarheim, I., Smedsrud, L., Ingvaldsen, R., and Nilsen, F.: Loss of sea ice during winter north of Svalbard, *Tellus A*, 66, 23933, doi:10.3402/tellusa.v66.23933, 2014. 4056
- Pavlov, A., Tverberg, V., Ivanov, B., Nilsen, F., Falk-Petersen, S., and Granskog, M.: Warming of Atlantic water in two West Spitsbergen fjords over the last century (1912–2009), *Polar Res.*, 32, 11206, doi:10.3402/polar.v32i0.11206, 2013. 4054
- 25 Styszyńska, A.: Ice condition in Hornsund and its foreshore (SW Spitsbergen) during winter season 2007/2008, *Problemy Klimatologii Polarnej*, 19, 247–267, 2009. 4046
- Styszyńska, A. and Kowalczyk, M.: Ice condition in Hornsund and its foreshore (SW Spitsbergen) during winter season 2005–2006, *Problemy Klimatologii Polarnej*, 17, 147–158, 2007. 4046
- 30 Styszyńska, A. and Rozwadowska, A.: Ice condition in Hornsund and its foreshore (SW Spitsbergen) during winter season 2006/2007, *Problemy Klimatologii Polarnej*, 18, 141–160, 2008. 4046

### Sea ice cover in Isfjorden and Hornsund 2000–2014 by using remote sensing

S. Muckenhuber et al.

Title Page

Abstract

Introduction

Conclusions

References

Tables

Figures

◀

▶

◀

▶

Back

Close

Full Screen / Esc

Printer-friendly Version

Interactive Discussion



TCD

9, 4043–4066, 2015

**Sea ice cover in Isfjorden and Hornsund 2000–2014 by using remote sensing**

S. Muckenhuber et al.

Title Page

Abstract

Introduction

Conclusions

References

Tables

Figures



Back

Close

Full Screen / Esc

Printer-friendly Version

Interactive Discussion





## Sea ice cover in Isfjorden and Hornsund 2000–2014 by using remote sensing

S. Muckenhuber et al.

Title Page

Abstract

Introduction

Conclusions

References

Tables

Figures

◀

▶

◀

▶

Back

Close

Full Screen / Esc

Printer-friendly Version

Interactive Discussion



**Table 2.** Calculated days of fast ice coverage (DFI) for Isfjorden and Hornsund between 2000 and 2014 for two different time periods. Total season refers to the entire sea ice season starting during autumn of the previous year and short season refers to 1 March until the end of the ice season, i.e. the time period when VIS/NIR images are available.  $\Delta$  describes the difference between entire and short season.

[DFI] year	total season	Isfjorden short season	$\Delta$	total season	Hornsund short season	$\Delta$
2000	–	46.0	–	–	56.7	–
2001	–	33.8	–	–	54.3	–
2002	–	52.2	–	–	53.6	–
2003	–	43.1	–	–	53.5	–
2004	–	70.7	–	–	59.9	–
2005	–	55.4	–	–	56.0	–
2006	19.4	9.5	9.9	25.8	25.8	0
2007	19.3	14.1	5.2	51.1	40.1	11
2008	28.5	20.5	8	54.2	49.8	4.4
2009	61.6	49.8	11.8	71.4	51.4	20
2010	34.9	24.8	10.1	53.6	47.4	6.2
2011	68.7	32.2	36.5	76.1	44.9	31.2
2012	16.9	12.8	4.1	2.5	2.0	0.5
2013	22.7	19.0	3.7	49.9	47.0	2.9
2014	18.0	13.2	4.8	2.5	0.4	2.1
mean $\pm$ SD	<b>32.2 <math>\pm</math> 18.5</b>	<b>33.1 <math>\pm</math> 18.2</b>	10.5 $\pm$ 9.6	<b>43.0 <math>\pm</math> 25.5</b>	<b>42.9 <math>\pm</math> 18.2</b>	8.7 $\pm$ 9.9

## Sea ice cover in Isfjorden and Hornsund 2000–2014 by using remote sensing

S. Muckenhuber et al.

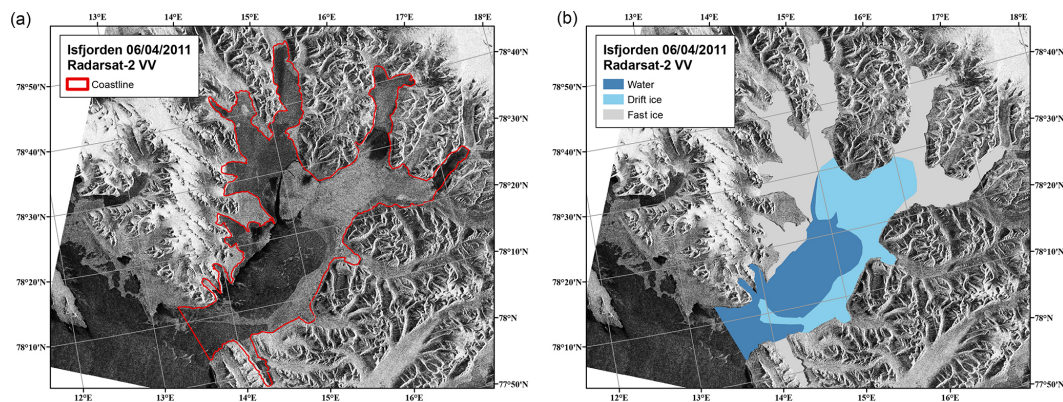


**Figure 1.** Radsat-2 image of Isfjorden taken on 6 April 2011 as shown in ArcGIS with adjusted Symbology (a) before and (b) after analysis of sea ice expert.

[Title Page](#)[Abstract](#)[Introduction](#)[Conclusions](#)[References](#)[Tables](#)[Figures](#)[◀](#)[▶](#)[◀](#)[▶](#)[Back](#)[Close](#)[Full Screen / Esc](#)[Printer-friendly Version](#)[Interactive Discussion](#)

## Sea ice cover in Isfjorden and Hornsund 2000–2014 by using remote sensing

S. Muckenhuber et al.

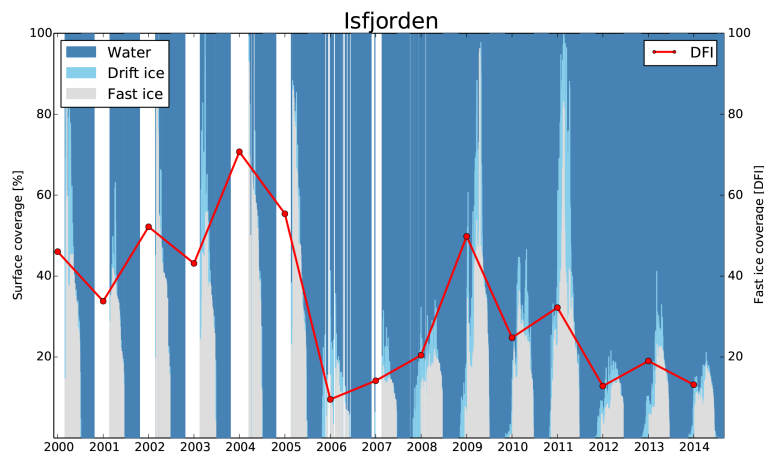


**Figure 2.** Surface coverage of Isfjorden between 2000 and 2014 divided into “Fast ice”, “Drift ice” and open “Water” by sea ice expert. Total area = 2487.6 km<sup>2</sup> (defined with Landsat image from 19 September 2013). White gaps occur when no satellite data was available. The red dots display the days of fast ice coverage (DFI) values of the short season as shown in Table 2.

[Title Page](#)
[Abstract](#)
[Introduction](#)
[Conclusions](#)
[References](#)
[Tables](#)
[Figures](#)
[◀](#)
[▶](#)
[◀](#)
[▶](#)
[Back](#)
[Close](#)
[Full Screen / Esc](#)
[Printer-friendly Version](#)
[Interactive Discussion](#)

## Sea ice cover in Isfjorden and Hornsund 2000–2014 by using remote sensing

S. Muckenhuber et al.

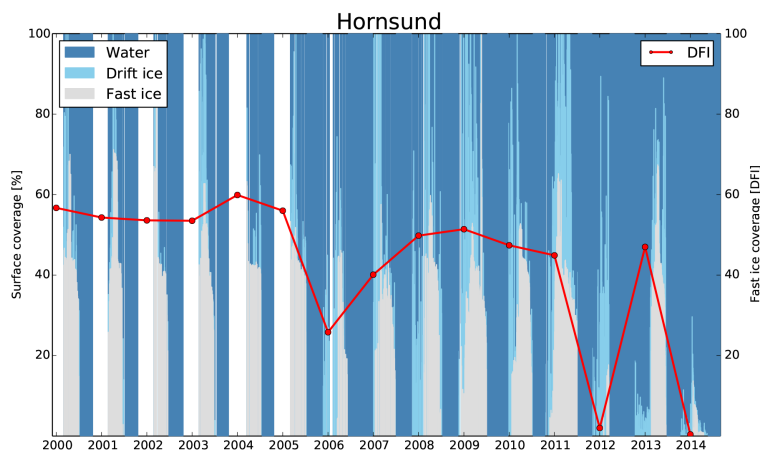


**Figure 3.** Surface coverage of Hornsund between 2000 and 2014 divided into “Fast ice”, “Drift ice” and open “Water” by sea ice expert. Total area = 324.0 km<sup>2</sup> (defined with Landsat image from 24 August 2013). White gaps occur when no satellite data was available. The red dots display the days of fast ice coverage (DFI) values of the short season as shown in Table 2.

Title Page

Abstract

Introduction

Conclusions

References

Tables

Figures

◀

▶

◀

▶

Back

Close

Full Screen / Esc

Printer-friendly Version

Interactive Discussion

## Sea ice cover in Isfjorden and Hornsund 2000–2014 by using remote sensing

S. Muckenhuber et al.

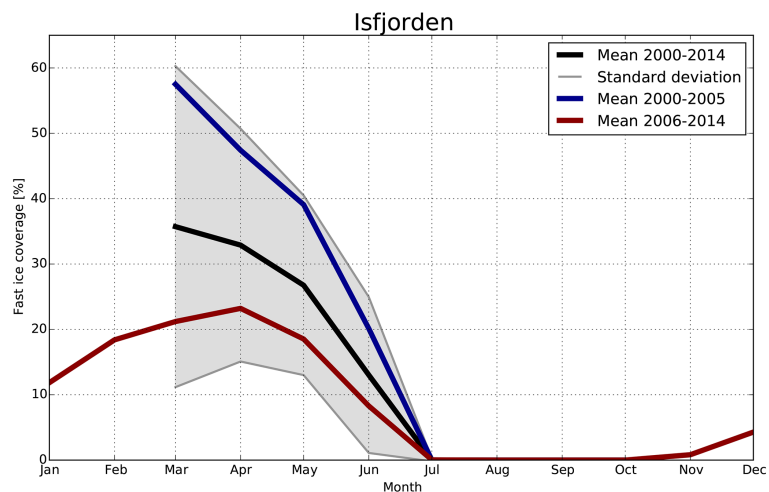


**Figure 4.** Monthly averaged fast ice coverage in Isfjorden shown for three time periods: 2000–2014 (mean in black and standard deviation in grey) 2000–2005 (blue) and 2006–2014 (red).

Title Page

Abstract

Introduction

Conclusions

References

Tables

Figures

◀

▶

◀

▶

Back

Close

Full Screen / Esc

Printer-friendly Version

Interactive Discussion

## Sea ice cover in Isfjorden and Hornsund 2000–2014 by using remote sensing

S. Muckenhuber et al.

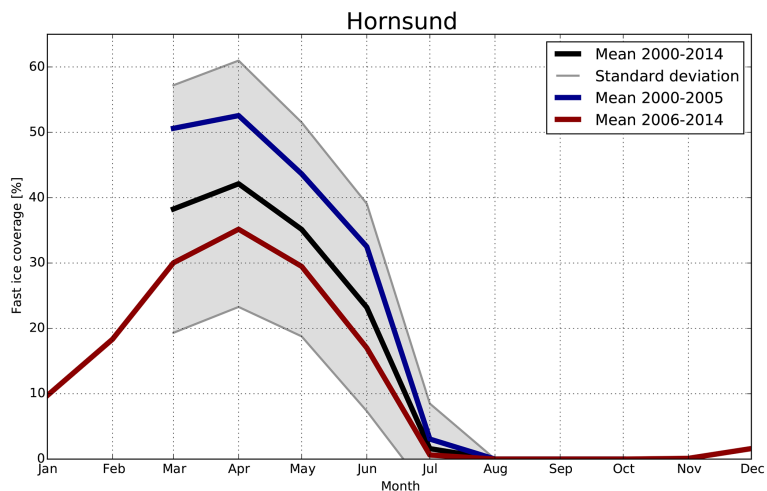


**Figure 5.** Monthly averaged fast ice coverage in Hornsund shown for three time periods: 2000–2014 (mean in black and standard deviation in grey) 2000–2005 (blue) and 2006–2014 (red).

[Title Page](#)[Abstract](#)[Introduction](#)[Conclusions](#)[References](#)[Tables](#)[Figures](#)[◀](#)[▶](#)[◀](#)[▶](#)[Back](#)[Close](#)[Full Screen / Esc](#)[Printer-friendly Version](#)[Interactive Discussion](#)

## Sea ice cover in Isfjorden and Hornsund 2000–2014 by using remote sensing

S. Muckenhuber et al.

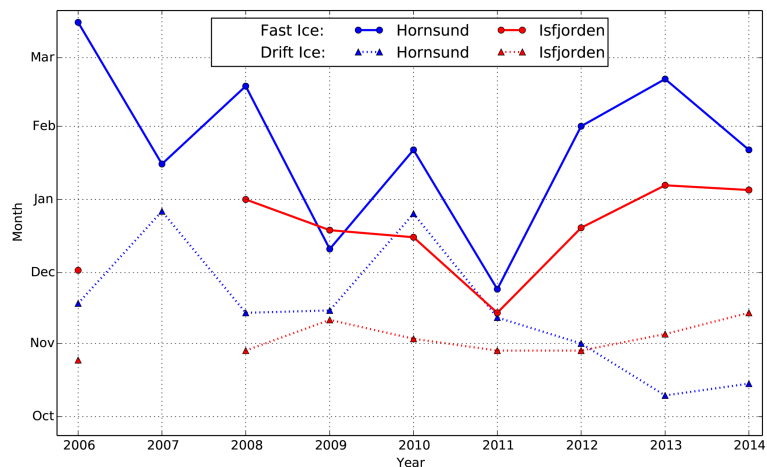


**Figure 6.** Onset of sea ice cover in Isfjorden and Hornsund. The years refer to the sea ice season, which starts during the previous year, meaning that January marks the beginning of the respective year. The triangles and dots mark the days with first appearance of drift and fast ice, i.e. the start of the sea ice season. Too few satellite images were available for Isfjorden in 2007 to give a reliable estimate.